Sedimentary Geology 216 (2009) 117–124

Contents lists available at ScienceDirect

Sedimentary Geology

journal homepage: www.elsevier.com/locate/sedgeo

High-resolution isotope stratigraphy of the Devonian–Carboniferous boundary in the Namur–Dinant Basin, Belgium

Karem Azmy [a,*], Edouard Poty [b], Uwe Brand [c]

[a] Department of Earth Sciences, Memorial University of Newfoundland, St. John's, NL, Canada, A1B 3X5
[b] Département de géologie, Unité de paléontologie animale et humaine, Université de Liège, Allée du 6 Août, Bâtiment B 18, B-4000 Liège-1, Belgium
[c] Department of Earth Sciences, Brock University, St. Catharines, ON, Canada, L2S 3A1

ARTICLE INFO

Article history:
Received 16 September 2008
Received in revised form 3 February 2009
Accepted 2 March 2009

Keywords:
Chemostratigraphy
Devonian–Carboniferous boundary
Namur–Dinant Basin
Belgium

ABSTRACT

The Devonian–Carboniferous (D–C) boundary sequence of the Namur–Dinant Basin in southern Belgium consists of marine platform carbonates. Global biostratigraphic correlation of the boundary has been a dilemma due to the absence of index conodont zones. Despite the scarcity of brachiopods, we managed to sample twenty-five calcitic shells from boundary beds at the Royseux-Gare section, to reconstruct biochemostratigraphic profiles of oxygen-, carbon- and strontium-isotopes for correlations with established global counterparts. The $\delta^{18}O$ and $\delta^{13}C$ values of the well-preserved shells range from −7.8 to −6.3‰ VPDB (−7.2 ± 0.4, $n = 25$) and from +1.1 to +2.4‰ VPDB (1.8 ± 0.3, $n = 25$), respectively. The shells also yielded $^{87}Sr/^{86}Sr$ ratios between 0.708185 and 0.708297. The Royseux isotope signatures are within the ranges documented for the global D–C boundary but their isotope profiles, however, show no significant shifts or excursions. Evaluation of the Royseux isotope profiles and correlation with their global counterparts may suggest a stratigraphic hiatus approximately from the middle *Siphonodella praesulcata* to the lower *Siphonodella sulcata* zones on the global D–C boundary conodont biostratigraphic scheme, while corresponding to the Hangenberg Event in Belgium.

© 2009 Elsevier B.V. All rights reserved.

1. Introduction

Geochemical studies have proven that well-preserved carbonates retain their primary stable-isotope and trace-element signatures that can be reliably utilized to study the paleo-environmental conditions (climate and oceanography) and construct high-resolution correlations of sequences from different depositional settings (e.g. Azmy et al., 1998, 1999; Veizer et al., 1999; Brand et al., 2004). This is an efficient technique particularly for sequences that have poor biostratigraphic resolution such as is the case of the Carboniferous–Devonian boundary (D–C) in the Namur–Dinant Basin of Belgium, where a stratigraphic hiatus spans the boundary (Paproth and Streel, 1984; van Steenwinkel, 1990). Brachiopod shells are among the ideal materials for geochemical investigation since they occur, although rarely, in the marine sequence of the current study and their low-Mg calcite, in many cases, retains the encrypted primary geochemical signatures in equilibrium with ambient seawater (cf. Veizer et al., 1999). Despite the scarcity of brachiopods in the investigated sequence, the sampled shells exhibit a high degree of preservation.

The main objectives of the current study are:

(1) to present biochemostratigraphic trends (C-, O-, and Sr-isotopes) for the Devonian–Carboniferous boundary sequence in the Namur–Dinant Basin using preserved brachiopods,
(2) to compare the biochemostratigraphic data from the Namur–Dinant Basin with those from the Devonian–Carboniferous GSSP trend of La Serre in the Montagne Noire (France) and other auxiliary sequences for possible refined global chemocorrelation.

2. Study area and stratigraphic dilemma

The Devonian–Carboniferous (D–C) sequence of southern Belgium occurs in the northwestern part of the Rheno–Hercynian Fold Belt (Hance et al., 2001) and during deposition was a part of the Namur–Dinant Basin (Fig. 1). The sequence spans the Devonian (Strunian)–Carboniferous (Tournaisian) boundary and consists, from base to top, of two main formations: (1) the Etroeungt Limestone and its lateral equivalent the Comblain-au-Pont Formation, and (2) the Hastière Formation (Paproth et al., 1983; Hance and Poty, 2006). The current study is focused on the boundary section at the Royseux-Gare, which is located in the Condroz sedimentation area (Figs. 1 and 2).

* Corresponding author. Tel./fax: +1 709 737 2589.
E-mail address: kazmy@mun.ca (K. Azmy).

0037-0738/$ – see front matter © 2009 Elsevier B.V. All rights reserved.
doi:10.1016/j.sedgeo.2009.03.002

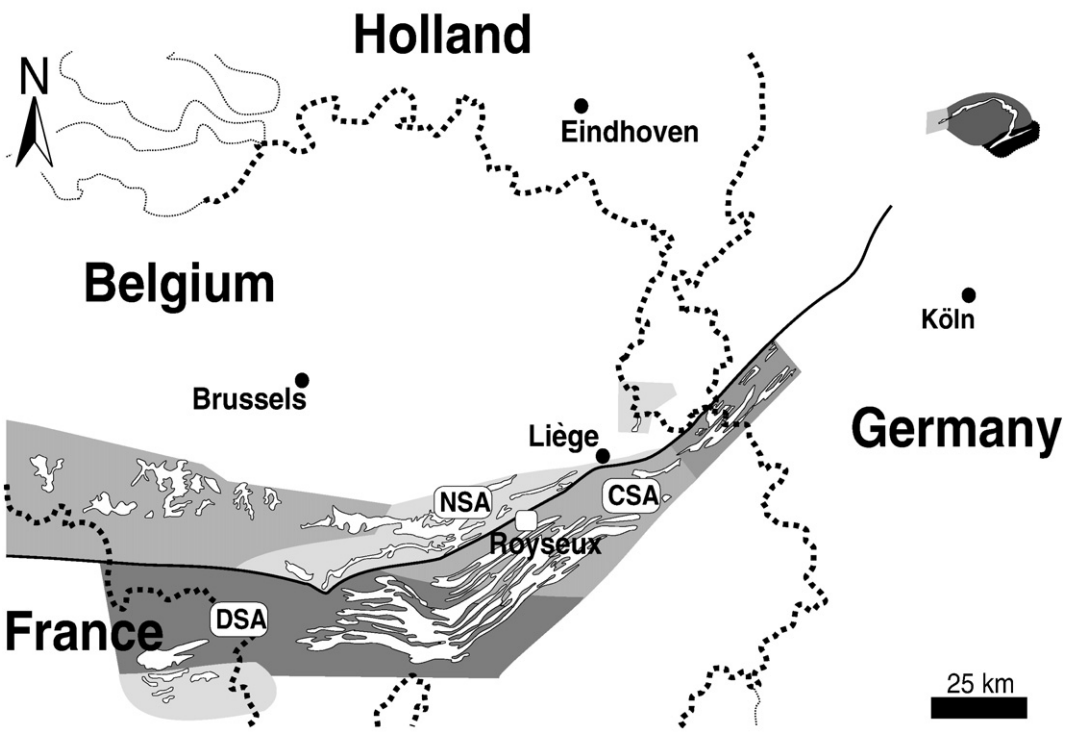

Fig. 1. Map of the study area showing the location of the investigated Royseux-Gare section and distribution of the Uppermost Devonian (Strunian) and Lower Carboniferous deposits in the Namur–Dinant Basin of southern Belgium. DSA, Dinant; NSA, Namur; and CSA, Condroz.

The D–C boundary is defined by the entry of the conodont *Siphonodella sulcata* in the lineage of *Siphonodella praesulcata* to *S. sulcata* in a section at La Serre, France (Paproth et al., 1991). Unfortunately, these conodonts are never found in the rather shallow carbonate platform facies of the Franco-Belgian Basin that includes the study area, where the oldest record of siphonodellid conodonts (*Siphonodella duplicata*)

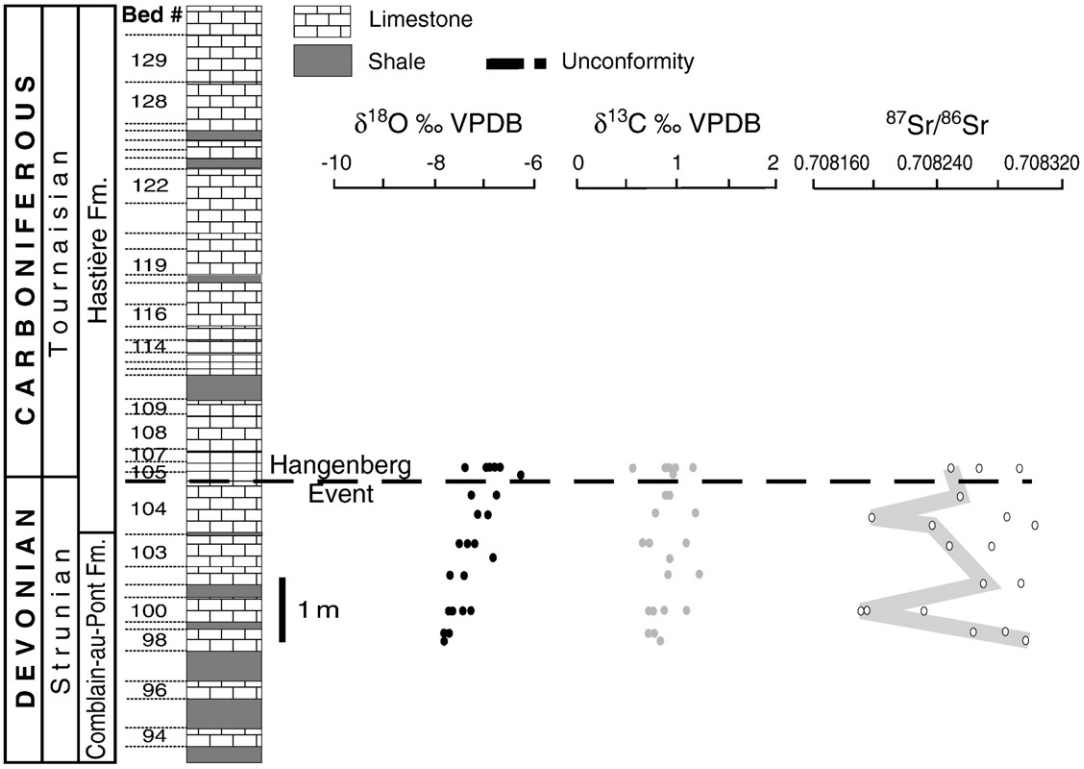

Fig. 2. Schematic diagram showing the stratigraphic log of the investigated Royseux-Gare section, including the Comblain-au-Pont (Etroeungt Limestone) and the Hastière formations, and the carbon-, oxygen- and strontium-isotope profiles. Grey line on the Sr-isotope graph represents the pattern of least radiogenic values.

is from the Anseremme railway section (the neostratotype for the base of the Tournaisian–Hastarian Substage), about 9 m above the base of the Hastière Formation (van Steenwinkel, 1988; Webster and Groessens, 1991). The base of the Tournaisian was suggested to correlate with the base of the "unilocular foraminifer zone" (MFZ1 Zone, Poty et al., 2006 and reference therein), which is relatively well correlated with the base of the *S. sulcata* Zone.

In Germany, the Hangenberg Event sensu stricto (Walliser, 1984) at the middle *S. praesulcata* condont Subzone, which is marked by the transgressive Hangenberg Black Shale (HBS), was correlated with the top of the Etroeungt limestones (Comblain-au-Pont Formation) and the conodont middle *S. praesulcata* Subzone (Figs. 2 and 3) and the highstand systems tract of the sequence has been suggested to correlate with the middle member of the Tournaisian Hastière Formation (Hance et al., 2001; Thorez et al., 2006). If this interval corresponds to the disappearance of many marine taxa in the deep environments, it had likely no influence on the shallow-water faunas, which reached at the same time their maximum development and subsequently disappeared during the sea-level fall correlated with the Hangenberg sandstone (Poty, 1999).

In the Namur–Dinant Basin, where shallow-water platform deposits dominate, the Hangenberg extinction event corresponds to a short sea-level fall correlated with the Hangenberg Sandstone and marked by a stratigraphic hiatus in the carbonate sequence (Poty, 1999). However, the event is usually assigned to a stratigraphic level near the base of the Hastière Formation (Fig. 2) and marked by the last occurrence of the foraminifera *Quasiendothyra*, corals of the RC0 Zone, stromatoporoids and phacopid trilobites (Poty, 1999).

In the Royseux-Gare section, the base of the Hastière Formation is marked by the base of Bed 104, which is separated from Bed 103 of the Comblain-au-Pont Formation by a 5 cm-thick shale interbed (Fig. 2). The extinction event is suggested between beds 104 and 105, which correlate with the last appearance of the *Quasiendothyra* and phacopids. The first post-event corals *Conilophyllum priscum* and *Kizilia kremersi* (RC1 Zone) were found in bed 106. Both foraminifers (MFZ1 Zone) and the first *S. duplicata* are present above bed 109 of the Royseux sequence (cf. Poty et al., 2006 and references therein).

Accordingly, the global correlation of the Devonian–Carboniferous transitional beds in the study area is still difficult and further work needs to be done to achieve this goal. This makes the stable-isotope stratigraphy a potential tool for resolving the dilemma, particularly because the Devonian–Carboniferous transition was a time interval of potential variations in the geochemical signatures of the primary marine carbonates (Brand et al., 2004) that were likely caused by dramatic paleo-environmental changes such as the Hangenberg Event sensu stricto post-event (e.g. Caplan and Bustin, 1999; Poty, 1999; Streel et al., 2000; Caplan and Bustin, 2001).

Compilation of isotopic data of well-preserved calcitic brachiopod shells from the sequences of the GSSP at La Serre (Montagne Noire, France) and other counterparts (cf. Brand et al., 2004), such as the Glen Park Formation and Louisiana Limestone of Missouri and the Wocklum Limestone at Wocklum, Germany (Kürschner et al., 1993; Bruckschen et al., 1995, 1999; Bruckschen and Veizer, 1997) and those of some near-micritic limemuds and preserved phosphatic conodonts from the Carnic Alps (Kaiser et al., 2006, 2008) show drastic changes in the trends of Sr-, C- and O-isotopes across the Devonian–Carboniferous boundary that can be potentially used for facilitating the global correlation of the Royseux-Gare sequence (Fig. 3).

3. Methods

Brachiopods are very rare across the Devonian–Carboniferous interval outcrops in the Namur–Dinant Basin of Belgium. About 29

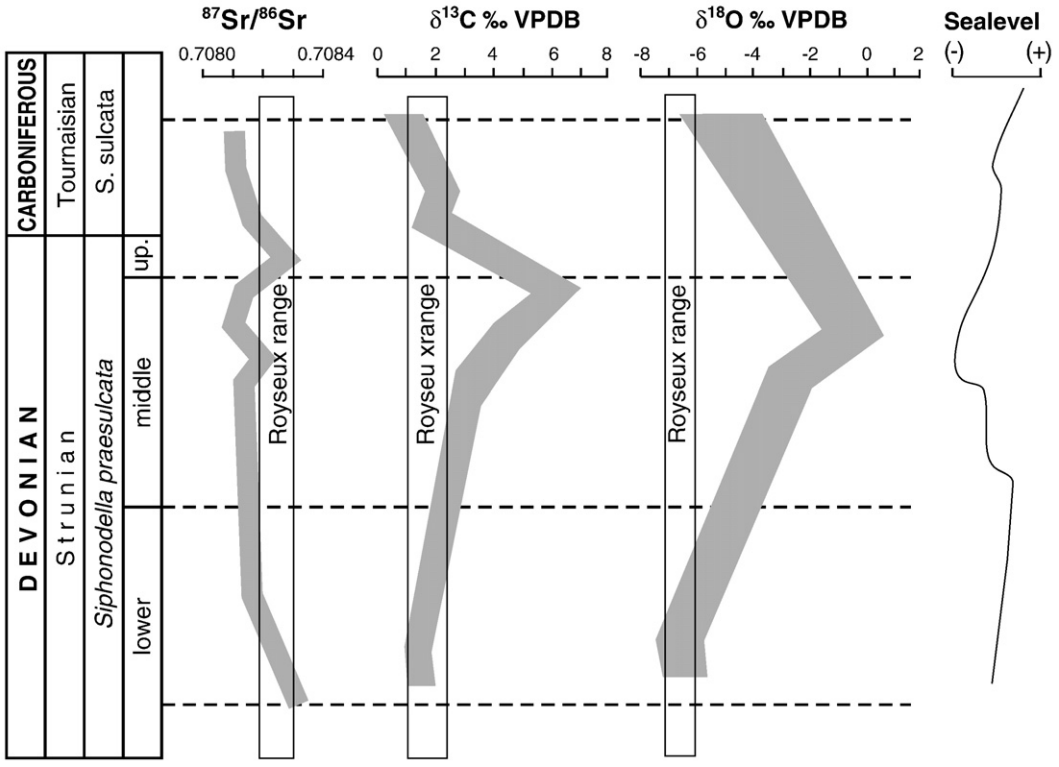

Fig. 3. Global trends for C-, O- and Sr-isotope variations across the Devonian–Carboniferous boundary and the approximate stratigraphic levels of the correlated conodont biozonation (modified after Brand et al., 2004 and references therein). The boxes represent the range of the Royseux-Gare isotope values.

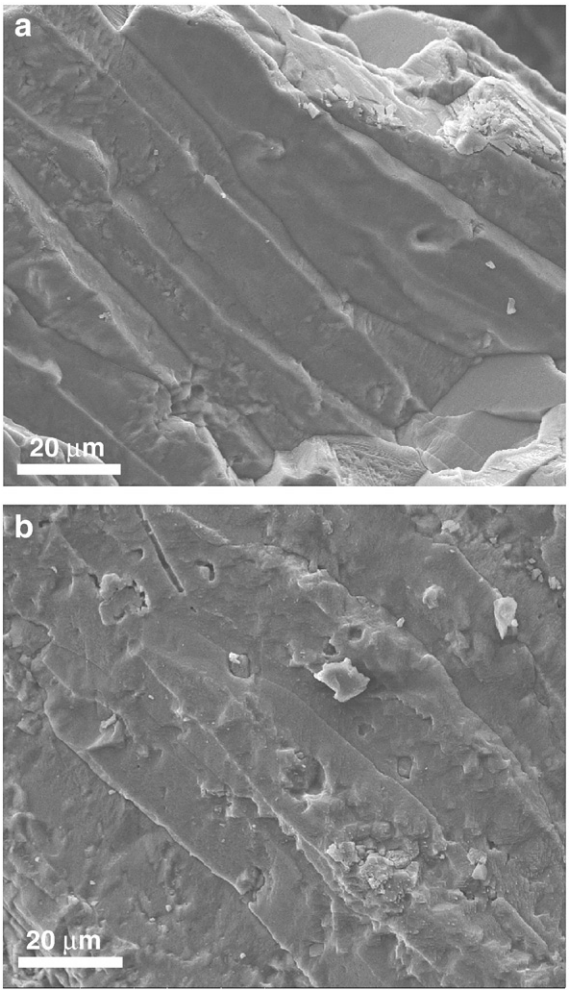

Fig. 4. Scanning Electron Microscopy photomicrographs of secondary shell layers of brachiopods from the investigated Royseux section showing (a) very good preservation with clean calcite-prism boundaries (Sample R104T-2) and (b) minor alteration (Sample R106-1) along some of the prisms. Both samples have comparable geochemical attributes (see Appendix A).

samples (25 brachiopods and 4 matrix) were collected at high-resolution (sampling interval ≤ 20 cm) from beds 98 to 106 (spanning the boundary) along the Royseux-Gare section (Fig. 2). Samples were cut into slabs and smashed to separate the brachiopod shells from the enclosing whole rock matrix. The secondary layers of the brachiopod shells usually spalled off the matrix, although occasionally traces of the primary layer needed to be removed by a dental pick, and the shell fragments were picked by forceps and cleaned in an ultrasonic bath. A shell fragment was randomly selected from each sample, coated with gold, and examined for the preservation of ultrastructure using a scanning electron microscope (SEM). The rest of each sample was powdered for chemical analyses.

About 200 μg of powder of each sample was reacted in an inert atmosphere with ultrapure concentrated (100%) orthophosphoric acid at 50 °C in a Thermo-Finnigan Gasbench II. The produced CO_2 was automatically delivered to a Thermo-Finnigan DELTA V plus isotope ratio mass spectrometer to be measured for C- and O-isotope ratios. Uncertainties of better than 0.1‰ (2σ) for the analyses were determined by repeated measurements of NBS-19 ($\delta^{18}O = -2.20$‰ and $\delta^{13}C = +1.95$‰ vs. VPDB) and L-SVECS ($\delta^{18}O = -26.64$‰ and $\delta^{13}C = -46.48$‰ vs. VPDB) as well as internal standards.

For elemental analyses, a subset of sample powder was digested in 0.075 M pure HNO_3 and analyzed for Ca, Mg, Sr, Mn and Fe (Coleman et al., 1989) using a HP 4500*plus* ICPMS at Memorial University of Newfoundland. The relative uncertainties of these measurements are better than 5%.

A subset of the preserved shells was selected for Sr-isotope analysis. About 1 mg of the powdered sample was dissolved in 2.5 N ultrapure HCl and, after evaporation, Sr was extracted with quartz glass exchange columns filled with Bio Rad AG50WX8 ion exchange resin. Finally, ~100 ng Sr was loaded on Re filaments using a Ta_2O_5–HNO_3–HF–H_3PO_4 solution. Measurements were performed with a Finnigan MAT 262 multicollector mass spectrometer at the Institut für Geologie, Mineralogie und Geophysik, Ruhr Universität, Bochum, Germany (e.g. Azmy et al., 1999 and references therein). Two standard reference materials were utilized as quality control of Sr-isotope ratio measurements, NBS 987 (mean $^{87}Sr/^{86}Sr = 0.709159 \pm 0.000004$, $n = 72$) and USGS EN-1 (mean $^{87}Sr/^{86}Sr = 0.710238 \pm 0.000005$, $n = 72$). The $^{87}Sr/^{86}Sr$ measurements were normalized to NBS 987 values bracketing the samples (0.710240) and corrected for deviation from value stated by McArthur (1994) to facilitate correlations with previous results from the D–C GSSP (Brand et al., 2004).

4. Results

Evaluation of the petrographic preservation of brachiopod shells is necessary before geochemical analyses in order to reveal hidden post-depositional diagenetic alteration in the shells, which might overprint the primary geochemical signatures. SEM images of the secondary layer of the sampled shells show mainly clean calcite prisms with smooth boundaries free of diagenetic dissolution features (Fig. 4a) except for very few samples that show some minor alterations (Fig. 4b).

The $\delta^{13}C$ and $\delta^{18}O$ values (Appendix A and Fig. 5) vary from +1.1 to +2.4‰ VPDB (1.8 ± 0.3, $n = 25$) and −7.8 to −6.3‰ VPDB (−7.2 ± 0.4, $n = 25$), respectively. These isotopic values are within the range documented for the Devonian–Carboniferous boundaries in Europe and N. America (Brand et al., 2004; Kaiser et al., 2008 and references therein). The shells have Sr, Mn and Fe contents (Appendix A and Fig. 6a,b) that vary from 1288 to 1531 ppm (1405 ± 87, $n = 5$), 23 to 51 ppm (32 ± 12, $n = 5$), and 219 to 670 ppm (374 ± 183, $n = 5$), respectively. The matrix samples ($n = 14$) are significantly enriched in Mn and Fe (353 ± 218 and 2262 ± 1614 ppm, respectively) and depleted in Sr (330 ± 52 ppm) compared with those of the preserved shells. The Sr-isotope ratios of the preserved shells ($n = 18$) vary from

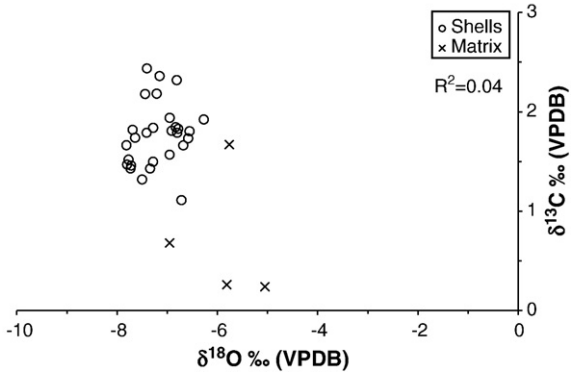

Fig. 5. Oxygen- vs. carbon-isotope values for the analyzed shells showing no diagenetic trend.

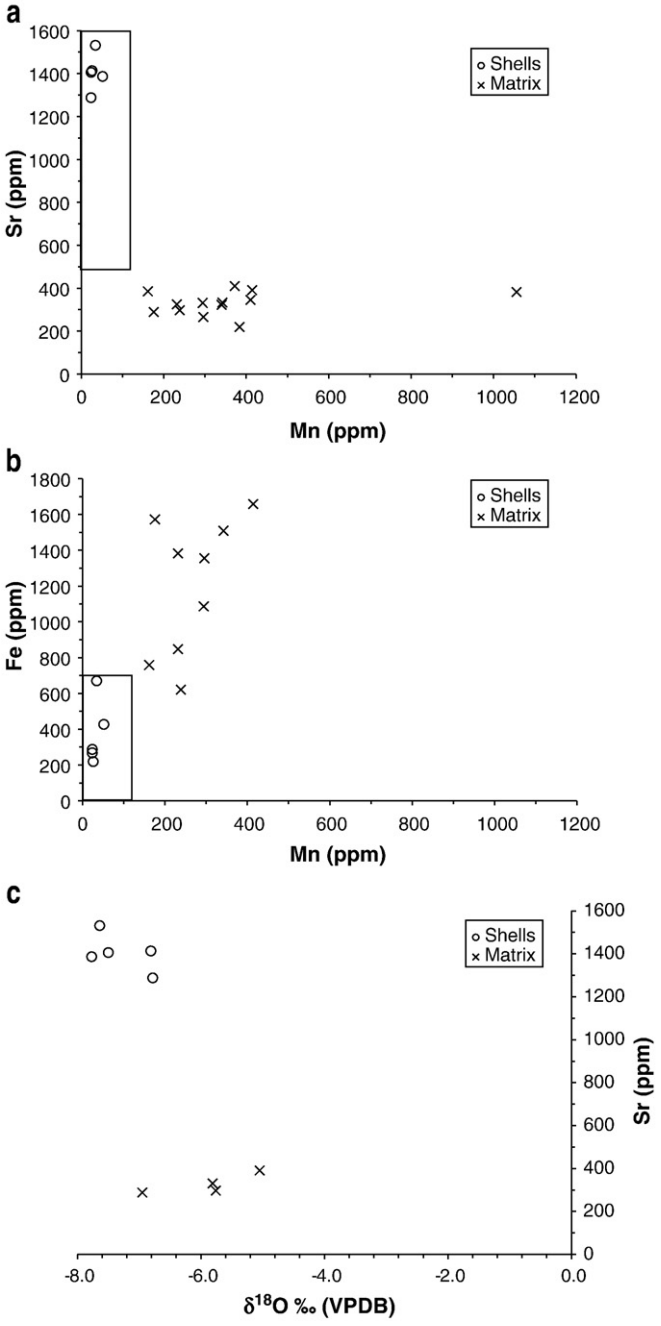

Fig. 6. Scatter diagrams of (a) Mn vs. Sr, (b) Mn vs. Fe, and (c) $\delta^{18}O$ vs. Sr for the analyzed brachiopod shells from the investigated section. The boxes in (a) and (b) represent the composition of modern brachiopods based on Lowenstam (1961) and Brand et al. (2003).

0.708185 to 0.708297 with a mean value of 0.708251 ± 0.000035 (Appendix A).

5. Discussion

5.1. Shell preservation

Brachiopod geochemistry has been extensively used as a proxy of the evolution of ancient oceans (e.g. Lowenstam, 1961; Veizer et al., 1986; Bates and Brand, 1991; Grossman et al., 1991; Wadleigh and Veizer, 1992; Wenzel and Joachimski, 1996; Azmy et al., 1998, 1999; Bruckschen et al., 1999; Mii et al., 1999; Veizer et al., 1999; Brand and Brenckle, 2001) and for high-resolution stratigraphic correlations of sequences from different sedimentary basins (e.g. Azmy et al., 1999; Veizer et al., 1999; Brand and Bruckschen, 2002; Brand et al., 2004). Articulated fossil brachiopod shells are among the ideal materials for this task since they precipitate their shells as low-Mg calcite that, to a certain degree, may resist alteration except for aggressive diagenetic processes (Brand and Veizer, 1980). The shell consists, in most cases, of three layers: a) the outermost (periostracum), which is organic and decomposes during fossilization, b) the primary layer is granular, few-micron thick calcite and always altered, and c) the secondary layer is prismatic low-Mg calcite that usually retains the original chemical signal of seawater (cf. Azmy et al., 1998; Veizer et al., 1999).

The pristine preservation of the analyzed shells is demonstrated by their SEM images (e.g. Azmy et al., 1998), which show stacked calcite prisms with no alteration features (Fig. 4). Their Sr, Mn and Fe contents are within the range of composition documented for their modern environment brachiopod shells (Fig. 6a,b) and there is also no diagenetic trend exhibited by $\delta^{18}O$ vs. Sr (Fig. 6c). Similarly, the $\delta^{18}O$ and $\delta^{13}C$ values (Fig. 5) show no correlation ($R^2 = 0.04$) and the composition of the matrix samples plot in all cases distinctively outside the values of the preserved shell populations (Fig. 6a,c). The $\delta^{18}O$ values of the studied shells are depleted relative to those of their modern (~0‰ VPDB) counterparts (Brand et al., 2003) due to the fact that the Paleozoic ocean waters were significantly depleted in ^{18}O compared with modern oceans but the fossil values are within the global range of the best preserved signatures documented for the late Devonian and early Carboniferous (Veizer et al., 1999; Came et al., 2007). Similarly, the $^{87}Sr/^{86}Sr$ ratios show insignificant correlations with the $\delta^{18}O$ and $\delta^{13}C$ values of the shells (Fig. 7a,b), thus suggesting no diagenetic overprint. This may imply that the investigated shells are geochemically well preserved, which is consistent with

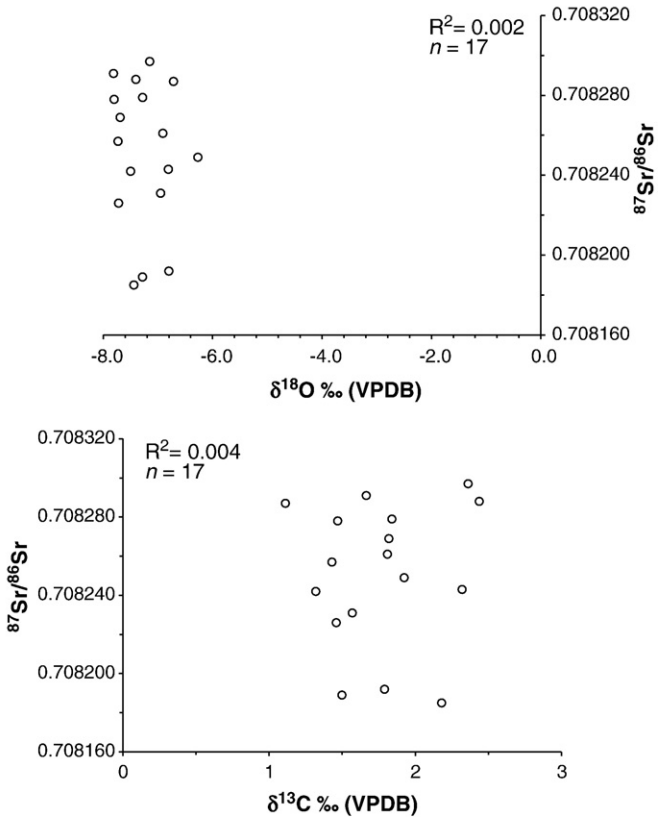

Fig. 7. Scatter diagrams of (a) $\delta^{18}O$ and (b) $\delta^{13}C$ vs. $^{87}Sr/^{86}Sr$ for the investigated shells showing insignificant correlations.

petrographic preservation and SEM images (e.g. Azmy et al., 1998; Veizer et al., 1999; Brand et al., 2004).

5.2. Global Devonian–Carboniferous chemostratigraphic profiles

The global chemostratigraphic profiles of the Devonian–Carboniferous boundary (Fig. 3) have been studied and refined by several authors (e.g. Bruckschen and Veizer, 1997; Mii et al., 1999; Veizer et al., 1999; Brand et al., 2004; Kaiser et al., 2006, 2008 and references therein). The global $\delta^{13}C$ profile, compiled from the GSSP (La Serre, France) and supplementary sections (Bruckschen and Veizer, 1997; Brand et al., 2004 their Fig. 7), show a distinct positive shift of ~5‰ (Fig. 3) rising from ~1.5‰ at the lower *S. praesulcata* to ~6.5 at the uppermost *S. praesulcata* Zone, immediately below the D–C boundary (*S. praesulcata–S. sulcata* boundary). A similar comparable positive shift of ~6‰ (Fig. 3) have been also documented in the $\delta^{18}O$ counterpart around the same stratigraphic level, rising from ~−7 to ~−1 at the same conodont zone levels, respectively (Brand et al., 2004 their Fig. 8). Preserved micritic limemud from equivalent sequences in the Carnic Alp provided a $\delta^{13}C$ profile with a comparable positive $\delta^{13}C$ shift of ~2–3‰ VPDB and the $\delta^{18}O$ profile of conodonts from the same interval yielded a similar shift of ~2‰ VSMOW approximately around the same stratigraphic level (Kaiser et al., 2008 their Fig. 8). Also, the global $^{87}Sr/^{86}Sr$ profile of the Devonian–Carboniferous boundary (Kürschner et al., 1993; Bruckschen and Veizer, 1997; Veizer et al., 1999; Brand et al., 2004 and references therein) exhibits a positive swing towards more radiogenic values at an approximate stratigraphic level correlated with the carbon- and oxygen-isotope shifts. The global least radiogenic values show an increase in the $^{87}Sr/^{86}Sr$ ratio from ~0.7081 in the lower and middle *S. praesulcata* to ~0.7083 at the uppermost *S. praesulcata* Subzone (immediately below the D–C boundary) and back to ~0.7081 at the *S. sulcata* Zone of the lowermost Carboniferous (Brand et al., 2004).

All isotopic shifts are also correlated with sea-level lowstands (Brand et al., 2004). Dramatic paleo-environmental changes (climatic and oceanographic) have been documented in association of the latest Devonian and earliest Carboniferous intervals (cf. Walliser, 1984; Streel et al., 2000). The terminal Devonian is marked by a significant global extinction event (Hangenberg Event sensu, Walliser, 1984) and glaciations that was associated with a major sea-level drops (Streel et al., 2000).

5.3. Dinant Devonian–Carboniferous chemostratigraphic profiles

The $\delta^{18}O$ values of the investigated Royseux-Gare section (−7.8 to −6.3‰ VPDB), which spans the D–C boundary in the Namur–Dinant Basin (Fig. 2), are significantly lower than their documented global counterparts (~−3.5 to +0.5‰ VPDB, Fig. 3) immediately below and above the boundary. The Royseux-Gare $\delta^{18}O$ profile (Fig. 2) shows no significant shifts around the unconformity surface (van Steenwinkel, 1990), which separates the Devonian strata from the carboniferous counterparts. This is consistent with the documented hiatus, based on the conodont biozonation and lithostratigraphy (Paproth and Streel, 1984; van Steenwinkel, 1990), placed between Bed 104 and Bed 105 (Fig. 2). The screening protocol of the investigated shells of the current studies proves a high degree of petrographic (ultrastructure) and geochemical preservation, suggesting highly reliable isotopic signatures. If so, comparison of the Royseux-Gare $\delta^{18}O$ values with their global counterparts (Fig. 3) may imply that the Devonian beds below the unconformity are possibly correlated with the lower *S. praesulcata* Zone on the global profile (Brand et al., 2004) and the Carboniferous beds immediately above the unconformity with the middle *S. sulcata* Zone.

Similarly, the Royseux-Gare $\delta^{13}C$ values (+1.1 to +2.4‰ VPDB) are lower than the global values (~+3 to +7‰ VPDB) immediately below and above the boundary (Fig. 3) and their profile across the unconformity surface, and along the investigated sequence, shows no isotopic excursions (Fig. 2). The high-resolution sampling sometimes from the top and bottom of each bed (Appendix A and Fig. 2), with intervals as small as 20 cm or even less in some beds (Fig. 2), most likely dismisses the issue of missing significant isotope shifts along the reconstructed profiles, particularly when the lack of the expected swing is associated with a documented stratigraphic hiatus. Although the $\delta^{13}C$ values of carbonate of the same age might at times vary from basin to basin depending on the local organic primary productivity in the basin, the $\delta^{13}C$ values of the investigated section are still within the range of the globally documented signatures (Brand et al., 2004 and references therein). The Royseux-Gare $\delta^{13}C$ values, particularly those below and above the unconformity surface (Fig. 2), may still suggest a possible global correlation at similar stratigraphic levels to those suggested by their $\delta^{18}O$ counterparts between the lower *S. praesulcata* Subzone and lower to middle *S. sulcata* Zone, respectively.

The Sr-isotope signatures of the preserved Royseux-Gare brachiopod shells from below and above the unconformity surface (Hangenberg Event) have narrow range of variations (~0.000100) and the pattern of their least radiogenic values (Fig. 2) shows no significant inflections compared with those exhibited by the global Sr-isotope profile in association with the C–D boundary (Fig. 3). However, the Royseux values are still within the range of global values documented for the lower *S. praesulcata* Subzone and at least the lower *S. sulcata* Zone (Fig. 3). This is also consistent with the correlations suggested by the Royseux $\delta^{18}O$ and $\delta^{13}C$ profiles.

6. Conclusions

Although brachiopods are extremely rare in the Devonian–Carboniferous boundary sections of southern Belgium, those of the current study, collected from the Royseux-Gare section, exhibit significant degree of petrographic and geochemical preservation as indicated by their SEM images and trace element contents.

Unlike the global stable-isotope profiles (C, O and Sr) of the Devonian–Carboniferous (GSSP) boundary, the Royseux-section counterparts exhibit no significant shifts or inflections along the unconformity surface. Thus, suggesting a stratigraphic hiatus likely caused by the Hangenberg Event, which is consistent with documented biostratigraphic evidences.

Correlation of the Royseux isotope profiles and the C-, O- and Sr-isotope values, particularly those below and above the unconformity surface of the Hangenberg Event, with their global counterparts may suggest a stratigraphic hiatus which may span approximately from the middle *S. praesulcata* to the lower *S. sulcata* zones on the global D–C boundary conodont biostratigraphic scheme.

Acknowledgements

We thank Drs. Ed Landing and Ganqing Jiang for their constructive reviews of this manuscript. Also, the efforts of Dr. Matthew Bennett and Mr. Paul Pearson are much appreciated. This project was funded by research grants from Memorial University of Newfoundland, Canada and Basel University, Switzerland (to K. Azmy), Université de Liège, Belgium (to E. Poty) and the Natural Sciences and Engineering Research Council of Canada (to U. Brand).

Appendix A

Geochemistry (trace element, isotopes) of brachiopods and whole rock (matrix) from the Devonian and Carboniferous interval at Royseux, Belgium. Sr-isotope values have been adjusted with respect to NBS 987 (0.710240) to facilitate correlation with previous other studies (Brand et al., 2004).

Appendix A

Sample ID	Location	Bed #	$CaCO_3$%	$MgCO_3$%	Sr (ppm)	Mn (ppm)	Fe (ppm)	$\delta^{13}C$ ‰VPDB	$\delta^{18}O$ ‰VPDB	$^{87}Sr/^{86}Sr \pm 2\sigma$	
R 98 T	Royseux	98	99.4	0.6	1387	51	427	1.5	−7.8		
R 98 T-2	Royseux						98	1.5	−7.8	0.708278	0.000007
R 98 T-3	Royseux	98						1.4	−7.7	0.708257	0.000007
R 98-1	Royseux	98						1.7	−7.8	0.708291	0.000007
R 98 T-M	Royseux	98	99.2	0.8	289	175	1572	0.7	−7.0		
R 98 T-M-2	Royseux		99.2	0.8	175	1572	289				
R 98-M	Royseux		95.7	4.3	340	4436	323				
R 100-1	Royseux	100	99.7	0.3	1531	34	670	1.7	−7.6	0.708189	0.000007
R 100-2	Royseux	100						2.2	−7.4	0.708185	0.000007
R 100-M	Royseux		98.7	1.3	1055	2657	382				
R 100-3	Royseux	100						1.5	−7.7	0.708226	0.000007
R 100-1-2	Royseux	100						1.5	−7.3		
R 102-T-1	Royseux	102						1.8	−7.7	0.708269	0.000007
R 102-1	Royseux	102						2.4	−7.4	0.708288	0.000007
R 102-M	Royseux		96.2	3.8	410	5530	345				
R 103 T-1	Royseux	103	99.8	0.2	1406	24	287	1.3	−7.5	0.708269	0.000007
R 103 T-2	Royseux	103						1.4	−7.3		
R 103 T	Royseux	103						2.2	−7.2	0.708242	0.000007
R 103-1	Royseux	103						1.8	−6.8		
R 103 T-M	Royseux	103	99.1	0.9	297	238	621	1.7	−5.8		
R 103 T-M-2	Royseux	103	99.1	0.9	238	621	297				
R 103 T-M-3	Royseux	103	98.8	1.2	296	1355	266				
R 103-M	Royseux	103	95.9	4.1	372	4064	409				
R 104 T-1	Royseux	104						1.8	−6.8	0.708192	0.000006
R 104 T-2	Royseux	104	99.7	0.3	1288	23	268	1.8	−6.8		
R 104 T-3	Royseux	104						1.8	−7.3	0.708279	0.000007
R 104	Royseux	104						2.4	−7.2	0.708297	0.000006
R 104-4-1	Royseux	104						1.6	−7.0	0.708231	0.000007
R 104 T-M	Royseux	104	98.9	1.1	391	414	1658	0.2	−5.1		
R 104 T-M-2	Royseux	104	98.9	1.1	414	1658	391				
R 104 T-M-3	Royseux	104	97.8	2.2	161	758	385				
R 104-1-M	Royseux	104	98.4	1.6	384	4186	220				
R 104-M	Royseux	104	98.2	1.8	342	1509	333				
R 105-1	Royseux	105						1.9	−6.3	0.708249	0.000007
R105-M	Royseux	105	98.6	1.4	231	1382	325				
R 106-1	Royseux	106	99.6	0.4	1413	26	219	2.3	−6.8	0.708243	0.000007
R 106-2	Royseux	106						1.8	−7.4		
R 106-3	Royseux	106						1.8	−6.9	0.708261	0.000007
R 106-4	Royseux	106						1.9	−7.0		
R 106	Royseux	106						1.1	−6.7	0.708287	0.000007
R 106-M	Royseux	106	98.5	1.5	331	294	1087	0.3	−5.8		
R 106-M	Royseux	106	98.5	1.5	294	1087	331				
R 106-M-2	Royseux	106	98.3	1.7	231	847	325				

T = top of bed and M = matrix.

References

Azmy, K., Veizer, J., Bassett, M.G., Copper, P., 1998. Oxygen and carbon isotopic composition of Silurian brachiopods: implications for seawater isotopic composition and glaciation. Geol. Soc. Am. Bull. 110, 1499–1512.

Azmy, K., Veizer, J., Wenzel, B., Bassett, M.G., Copper, P., 1999. Silurian strontium isotope stratigraphy. Geol. Soc. Am. Bull. 111, 475–483.

Bates, N.R., Brand, U., 1991. Environmental and physiological influences on isotopic and elemental compositions of brachiopod shell calcite: implications for the isotopic evolution of Paleozoic oceans. Chem. Geol., Isot. Geosci. Sect. 94, 67–78.

Brand, U., Veizer, J., 1980. Chemical diagenesis of a multicomponent carbonate system: 1. Trace elements. J. Sediment. Petrol. 50, 1219–1236.

Brand, U., Brenckle, P., 2001. Chemostratigraphy of the Mid-Carboniferous boundary global stratotype section and point (GSSP), Bird Spring Formation, Arrow Canyon, Nevada, USA. Paleogeogr. Paleoclimatol. Paleoecol. 165, 321–347.

Brand, U., Bruckschen, P., 2002. Correlation of the Askyn River section, southern Urals, Russia with the Mid-Carboniferous boundary GSSP, Bird Spring Formation, Arrow Canyon, Nevada, USA: implications for global paleoceanography. Palaeogeogr. Palaeoclimatol. Palaeoecol. 184, 177–193.

Brand, U., Logan, A., Hiller, N., Richardson, J., 2003. Geochemistry of modern brachiopods: applications and implications for oceanography and paleoceanography. Chem. Geol. 198, 305–334.

Brand, U., Legrand-Blain, M., Streel, M., 2004. Biochemostratigraphy of the Devonian–Carboniferous boundary global stratotype section and point, Griotte Formation, La Serre, Montagne Noire, France. Palaeogeogr. Palaeoclimatol. Palaeoecol. 205, 337–357.

Bruckschen, P., Veizer, J., 1997. Oxygen and carbon isotopic composition of Dinantian brachiopods: paleoenvironmental implications for the Lower Carboniferous of Western Europe. Paleogeogr. Paleoclimatol. Paleoecol. 132, 243–264.

Bruckschen, P., Bruhn, F., Veizer, J., Buhl, D., 1995. $^{87}Sr/^{86}Sr$ isotopic evolution of lower Carboniferous seawater: Dinantian of western Europe. Sediment. Geol. 100, 63–81.

Bruckschen, P., Oesmann, S., Veizer, J., 1999. Isotope stratigraphy of the European Carboniferous: proxy signals for ocean chemistry, climate and tectonics. Chem. Geol. 161, 127–163.

Came, R.E., Eiler, J.M., Veizer, J., Azmy, K., Brand, U., Weidman, C.R., 2007. Coupling of surface temperatures and atmospheric carbon dioxide concentrations during the Palaeozoic Era. Nature 449, 198–201.

Caplan, M.L., Bustin, R.M., 1999. Devonian–Carboniferous Hangenberg mass extinction event, widespread organic-rich mudrock and anoxia: causes and consequences. Paleogeogr. Paleoclimatol. Paleoecol. 148, 187–207.

Caplan, M.L., Bustin, R.M., 2001. Palaeoenvironmental and palaeoceanographic controls on black, laminated mudrock deposition; example from Devonian–Carboniferous strata from Alberta, Canada. Sediment. Geol. 145, 45–72.

Coleman, M.L., Walsh, J.N., Benmore, R.A., 1989. Determination of both chemical and stable isotope composition in milligram-size carbonate samples. Sediment. Geol. 65, 233–238.

Grossman, E.L., Zhang, C., Yancey, T.E., 1991. Stable isotope stratigraphy from brachiopods in Pennsylvanian (Upper Carboniferous) shales of Texas. Geol. Soc. Amer. Bull. 103, 953–965.

Hance, L., Poty, E., 2006. Hastarian. In: Dejonghe, L. (Ed.), Current Status of Chronostratigraphic Units Named From Belgium and Adjacent Areas. Geologica Belgica, vol. 9/1-2, pp. 111–116.

Hance, L., Poty, E., Devuyst, F.-X., 2001. Stratigraphie séquentielle du Dinantien type (Belgique) et corrélation avec le Nord de la France (Boulonnais, Avesnois). Bull. Soc. Geol. Fr. 172/4, 411–426.

Kaiser, S.I., Steuber, T., Becker, R.T., Joachimski, M.M., 2006. Geochemical evidence for major environmental changes at the Devonian–Carboniferous boundary in the Carnic Alps. Palaeogeogr. Palaeoclimatol. Palaeoecol. 240, 146–160.

Kaiser, S.I., Steuber, T., Becker, R.T., 2008. Environmental change during the Late Famennian and Early Tournaisian (Late Devonian–Early Carboniferous): implications from stable isotopes and conodont biofacies in southern Europe. Geol. J. 43, 241–260.

Kürschner, W., Becker, R.T., Buhl, D., Veizer, J., 1993. Strontium isotopes in conodonts: Devonian–Carboniferous transition, the northern Rhenish Slate Mountains Germany. Ann. Soc. Geol. Belg. 115, 595–621.

Lowenstam, H.A., 1961. Mineralogy, $^{18}O/^{16}O$ ratios, and strontium and magnesium contents of recent and fossil brachiopods and their bearing on the history of the ocean. J. Geol. 69, 341–360.

McArthur, J.M., 1994. Recent trends in strontium isotope stratigraphy. Terra Nova 6, 331–358.

Mii, H.-S., Grossman, E.L., Yancey, T.E., 1999. Carboniferous isotope stratigraphies of North America: implications for Carboniferous paleoceanography and Mississippian glaciation. Geol. Soc. Am. Bull. 111, 960–973.

The Devonian–Carboniferous Boundary. In: Paproth, E., Streel, M. (Eds.), Cour. Forschungsinst. Senckenberg, vol. 67, pp. 1–258.

Paproth, E., Conil, R., Bless, M.J.M., Boonen, P., Carpentier, N., Coen, M., Delcambre, B., Deprijck, C.H., Deuzon, S., Dreesen, R., Groessens, E., Hance, L., Hennebert, M., Hibo, D., Hahn, G.R., Hislaire, O., Kasig, W., Laloux, M., Lauwers, A., Lees, A., Lys, M., Op de Beek, K., Overlau, P., Pirlet, H., Poty, E., Ramsbottom, W., Streel, M., Swennen, R., Thorez, J., Vanguestaine, M., van Steenwinckel, M., Vieslet, J.L., 1983. Bio- and Lithostratigraphic subdivisions of the Dinantian in Belgium, a review. Ann. Soc. Geol. Belg. 106, 185–239.

Paproth, E., Feist, R., Flajs, G., 1991. Decision on the Devonian–Carboniferous boundary stratotype. Episodes 14, 331–335.

Poty, E., 1999. Famennian and Tournaisian recoveries of shallow water Rugosa following late Frasnian and late Strunian major crises, southern Belgium and surrounding areas, Hunan (South China) and the Omolon region (NE Siberia). Paleogeogr. Paleoclimatol. Paleoecol. 145, 11–26.

Poty, E., Devuyst, F.-X., Hance, L., 2006. Upper Devonian and Mississippian foraminiferal and rugose coral zonation of Belgium and Northern France: a tool for Eurasian correlations. Geol. Mag. 143, 829–857.

Streel, M., Caputo, M.V., Loboziak, S., Melo, J.H.G., 2000. Late Frasnian– Famennian climates based on palynomorph analyses and the question of the Late Devonian glaciations. Earth-Sci. Rev. 52, 121–173.

Thorez, J., Dreesen, R., Streel, M., 2006. Famennian. In: Dejonghe, L. (Ed.), Current Status of Chronostratigraphic Units Named From Belgium and Adjacent Areas. Geologica Belgica, vol. 9/1-2, pp. 27–45.

van Steenwinkel, M., 1988. The sedimentary history of the Dinant Platform during the Devonian–Carboniferous transition. PhD. Thesis, University of Leuven, 173 pp.

van Steenwinkel, M., 1990. Sequence stratigraphy from "spot" outcrops — example from carbonate-dominated setting: Devonian–Carboniferous transition, Dinant synclinorium (Belgium). Sediment. Geol. 69, 259–280.

Veizer, J., Fritz, P., Jones, B., 1986. Geochemistry of brachiopods: oxygen and carbon isotopic records of Paleozoic oceans. Geochim. Cosmochim. Acta 50, 1679–1696.

Veizer, J., Ala, D., Azmy, K., Bruckschen, P., Bruhn, F., Buhl, D., et al., 1999. $^{87}Sr/^{86}Sr$, $\delta^{18}O$ and $\delta^{13}C$ evolution of Phanerozoic seawater. Chem. Geol. 161, 59–88.

Wadleigh, M.A., Veizer, J., 1992. $^{18}O/^{16}O$ and $^{13}C/^{12}C$ in Lower Paleozoic articulate brachiopods: implications for the isotopic composition of seawater. Geochim. Cosmochim. Acta 56, 431–443.

Walliser, O.H., 1984. Pleading for a natural D/C boundary. Cour. Forschungsinst. Senckenberg 67, 241–246.

Webster, G.D., Groessens, E., 1991. Conodont subdivisions of the Lower Carboniferous. In: Brenckle, P.L., Manger, W.L. (Eds.), International Correlation and Division of the Carboniferous System. Courier Forschunginstitut senckenberg, vol. 130, pp. 31–40.

Wenzel, B., Joachimski, M.M., 1996. Carbon and oxygen isotopic composition of Silurian brachiopods (Gotland, Sweden): paleoceanographic implications. Paleogeogr. Paleoclimatol. Paleoecol. 122, 143–166.